— 12 —

X-ray imaging with collimators, masks and grids

Gordon J. Hurford[I]

Abstract

The basic principles of X-ray and γ-ray imaging for astronomy with non-focusing optics are briefly reviewed. Specific topics include coded masks, and bigrid and multigrid collimators. The advantages and limitations of the various design options are discussed and illustrated with representative examples.

Introduction

At most wavelengths, imaging is based on optics that use reflection or refraction to focus the incident light on a multi-element detector. This provides a direct image of the source. At very short wavelengths (≤ 0.1 µm), however, the physics of the reflection or refraction can render this impractical and other techniques have been employed for hard X-rays and γ-rays (e.g., Ramsey et al 1993). This is particularly true for imaging with high angular resolution ($\approx 4''$ to $6'$) and/or over a large ($\geq 1^\circ$) field of view (FOV).

For imaging beyond the range of focusing optics, it is necessary to resort to collimators, masks and/or grids. By selectively blocking or transmitting incident photons depending on their direction of incidence, they rely on absorption or scattering rather than reflection or refraction to provide an imaging capability. They effectively transform the angular distribution of the incident radiation to either a spatial variation or a temporal variation in the detected photons (spatial or time modulation). Such systems are implemented as a single absorbing layer with apertures (mask), a pair of separated grids (bigrid collimator), or multiple grids (multigrid collimator).

A related approach uses a set of continuous blades oriented parallel to the desired direction of photon travel to restrict the photon transmission to a limited range of angles. Such *slat* or *Soller* collimators can be scanned across the field of view to provide limited angular resolution. They are also useful for coarsely constraining the X-ray FOV (for example to limit background). However, we will not consider them further here.

[I]Space Sciences Laboratory, University of California, Berkeley, USA

The possible configurations of collimator-based imagers are quite diverse and adaptable to a wide range of spacecraft constraints. The choice of collimation approach (single, bigrid or multigrid; temporal or spatial modulation) depends on design drivers such as the available mass and volume, type of attitude control (three-axis or spin stabilized); detector characteristics (particularly its spatial resolution); and the relative scientific importance of angular resolution, FOV and sensitivity. In addition, there are physics-driven constraints on possible combinations of energy range, FOV, angular resolution, and collimator length.

Single-grid systems

Single-grid systems have been used for imaging since long before the advent of modern astronomy. The *camera obscura* consists simply of a small pinhole in an opaque mask. It forms an (inverted) image of a bright object on a distant screen that is otherwise in shadow. The angular resolution of such a device is determined by the combination of single pinhole diffraction and the ratio of the diameter of the pinhole to its separation from the screen. Although originally used for making visible images, such optics can be used at any wavelength provided the pinhole is in a material that is opaque to the photons of interest. As a result, the principle can be applied to X-ray or γ-ray imaging. However, for the weak fluxes characteristic of astronomical sources it is not useful, since the only photons that are detected are those that pass though the pinhole whose size must be small to achieve high angular resolution. As a result, the sensitivity is profoundly limited.

Dicke (1968) overcame this limitation by using a *set* of randomly positioned pinholes in the mask that created a corresponding set of overlapping images (Figure 12.1). For simple sources, the original image can then be recovered by deconvolving the observed pattern. The effective area is now much larger since it is given by the total area of all the apertures that together can be up to ≈ 50 % of the frontal area of the instrument. There are many ways to choose the 'random' pattern of the apertures. One class of such patterns is the uniformly redundant array (URA) illustrated in Figure 12.2. Fenimore's (1980) analysis of a URA response showed the main peak of the angular response is still defined by the geometry of the individual apertures, while the point response function has flat sidelobes. Such URA masks have been extensively used for astronomical applications, most recently on *Swift* (Barthelemey et al 2000) and *INTEGRAL* (Ubertini et al 2003).

As might be expected, the FOV of such systems is given by the ratio of the detector and/or mask size to their separation. The resulting FOV can be quite large (up to ≈ 1 sr) and so enables simultaneous observation of multiple sources. This can be useful for example in survey or burst monitoring applications where the source location is not known a priori. An extensive set of references on coded aperture imaging can be found at http://astrophysics.gsfc.nasa.gov/cai/coded_bibl_short.html.

There are three downsides to imaging with coded masks, however. The first is that the detectors must have spatial resolution that is comparable to or better than the diameter of the mask apertures. This limits the options for detectors by placing a premium on the detector's spatial resolution. In addition to adding complexity and possibly compromising spectral resolution, the detector spatial resolution limits

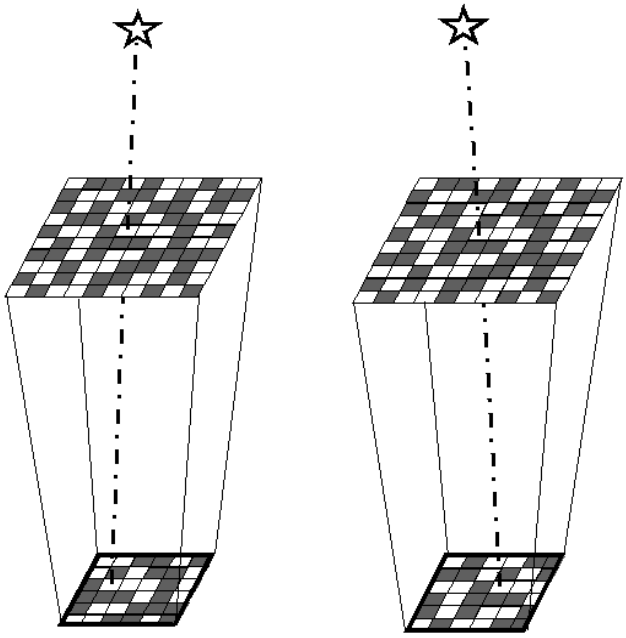

Figure 12.1: Schematic illustration of two identical pinhole arrays (top) casting their shadows on the corresponding detector (bottom). Note how the detected shadow patterns depend on the direction of the incident photon.

the angular resolution achievable by practical sized instrumentation to at best a few minutes of arc. While this may be acceptable for 'point-like' astronomical sources, it is a significant impediment to the use of URAs in solar applications, for example, where angular resolutions of a few seconds of arc are desirable. A second limitation, also relevant to solar applications, is that the response of URAs is degraded for extended sources. Fenimore (1980) provides a clear discussion of the modulation transfer function. The third consideration, in common with most indirect imaging techniques, is that the statistical noise in observations of a given source arises not only from background and its own statistics, but also from all other sources in the FOV. When background does not dominate, this can make it more difficult to detect weak sources in the presence of strong ones.

Bigrid collimators

The modulation collimator (Oda 1965) overcomes the coded mask's angular resolution limitations by replacing the single mask with two or more grids to form a *modulation collimator*. The grids in such systems consist of a large number of parallel X-ray opaque slats separated by X-ray transparent slits. This provides a way to decouple the achievable angular resolution from the spatial resolution of the

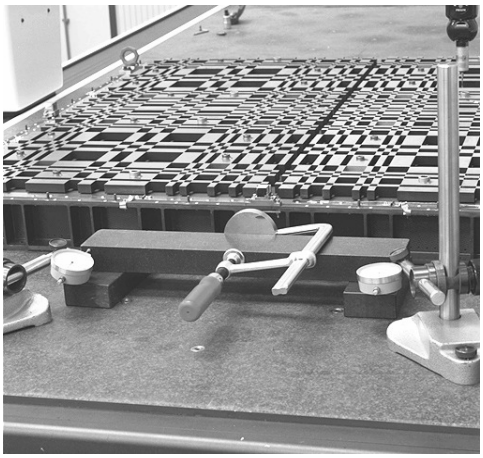

Figure 12.2: Uniformly redundant array mask on *INTEGRAL*/IBIS (adapted from http://integral.esac.esa.int).

detector which in turn opens the way to obtaining much higher angular resolution within a given instrument envelope.

Bigrid collimators fall into two broad classes: those that generate a spatial pattern in the transmitted photon flux that depends on their incident direction (spatial modulation) and those that impose a distinctive time-dependence on the transmitted photon flux (time modulation).

In a bigrid collimator using spatial modulation (sometimes called an imaging collimator), the pitch and/or orientation of the front and rear grids differ slightly so that they have slightly different spatial frequencies. As a result, for a given direction of incidence, the transmitted flux forms a large-scale Moiré pattern that has one or a few cycles across the detector (Figure 12.3). The phase of this Moiré pattern (i.e., the location of its maximum) depends sensitively (and periodically) on the incident photon direction, since it goes through a complete cycle with a change of photon direction given by the ratio of the average grid pitch to their separation. Although the Moiré pattern really consists of a large number of narrow stripes (corresponding to the grid pitch), it can be characterized by a detector whose spatial resolution needs to be good enough to see only its large-scale 'envelope'. Therefore the spatial resolution requirement on the detector is determined by the grid diameter, while the angular response of the collimator as a whole is determined by the much smaller grid pitch.

Alternatively, in a time-modulation collimator the top and bottom grids have identical pitch and orientation. If the photon direction with respect to the collimator changes as a function of time, the total transmitted flux also varies. Such time variations can be measured with a detector that need not have any spatial resolution whatsoever, and so it can be chosen or optimized on the basis of other considerations such as spectral resolution or high-energy response. Once again the

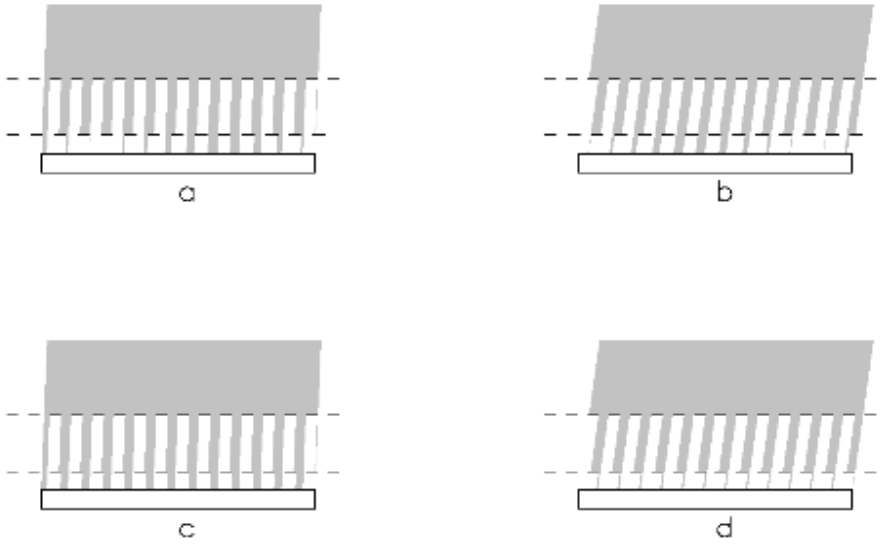

Figure 12.3: Schematic illustration of the transmission of bigrid collimators. The top panels show an imaging collimator for which the front and rear grids have slightly different pitch. For the two incident beam directions shown, the total transmission is about the same, but the location of the smoothed maximum transmission is significantly shifted. Alternatively, for the collimator shown in c and d, the grid pitches are identical. In this case, changing the incident direction affects the total detected flux.

angular resolution (defined as half the period of the response) is given by the ratio of half the grid-pitch to its separation.

Useful insights into the response of a bigrid collimator can be gained by considering the link between its transmission as a function of time (or position for an imaging collimator) and its transmission as a function of incident photon direction. If the slits and slats of the grids are of equal width, then this dependence has a quasi-triangular form. For a point source, the amplitude of this pattern is proportional to its strength, and the timing (or location in the case of spatial modulation) of the transmission maximum depends on source direction. Note that there is no information contained in the period since that is determined by the collimator's design and/or its changing orientation. Considering just the primary sinusoidal component of this pattern, it has been shown (Makishima et al 1977; Prince et al 1988) that the amplitude and phase of this pattern provide a direct measurement of a single Fourier component of the source distribution. Thus the response of a bigrid collimator is a precise mathematical analog to that of a pair of antennas in a radio interferometer, whose correlated signal also measures one such Fourier component. In both cases, images can be reconstructed from a set of Fourier component mea-

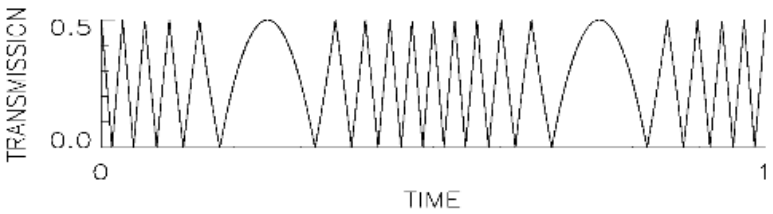

Figure 12.4: Schematic illustration of the time variation of the transmission of a bigrid rotation modulation collimator for a point source. The variations in the period of the modulation arise since, in the plane orthogonal to the grids, the source apparently moves with simple harmonic motion.

surements made at a large number of angular frequencies. This perspective on the response of a bigrid collimator greatly simplifies analyses of its angular response.

Although a time-modulation collimator uses the simpler detector system, some provision must be made to continually move the collimator with respect to the source so as to change the relative direction of the incident photons. This can be done by mechanically rocking the collimator, or by exploiting random motions (as with a badly pointed balloon platform). However, a common approach is to mount the collimator on a rotating spacecraft to form a rotating modulation collimator (RMC, Schnopper et al 1968). As the collimator rotates, its response over a limited range of angles is quasi-periodic (Figure 12.4). Over a half-rotation, however, the amplitude and phase of the modulation measures a set of Fourier components at a complete set of orientations at the spatial frequency determined by the grid pitch and separation. In the parlance of radio interferometry, the system measures spatial frequencies in a circle in the $u\nu$ (spatial frequency) plane in analogy to *Earth rotation synthesis*, except on a much more rapid timescale.

Early implementations of the rotating modulation collimator were used for surveys where the system detected point sources over a relatively wide FOV. Mertz (1968) also suggested using such collimators as imaging devices for extended sources. The most ambitious implementation to date of such an imager is *RHESSI* (Lin et al 2002) which uses a set of nine RMCs to image extended solar flare X-ray and γ-ray sources (Hurford et al 2002), achieving angular resolution as high as $2.3''$. The effectiveness of multiple RMCs in characterizing extended sources is based on the fact that a bigrid collimator cannot modulate X-rays from a source whose angular width is much larger than the collimator resolution. As a result, comparison of the modulation amplitude among collimators with different angular resolution can provide an accurate measurement of source size (e.g., Schmahl and Hurford 2002).

One measure of the performance of an RMC as an imager is the dynamic range of its images, i.e., the ratio of the brightest source in the FOV to the faintest credible feature. The dynamic range can be limited by any of three broad factors. First, a typical set of RMCs measures only a few dozen to a few hundred independent Fourier components, each of which is fully represented by a single complex

number. Since the number of observables is so limited, there is an unavoidable limitation on the complexity of the images that can be reconstructed. Second, photon statistics can be a limitation in both astrophysical and solar observations. This translates directly into a statistical uncertainty in each visibility that again limits the achievable dynamic range. Third, as with any instrument, there are inevitable calibration uncertainties that constrain the accuracy of each measurement. In practice any one (or more) of these factors can be the limiting factor, depending on the circumstances.

Although bigrid collimators can provide higher angular resolution than single-mask systems, this comes at some disadvantage in terms of sensitivity. In particular, the nominal average relative transmission of bigrid collimators is ≈ 25 %, compared to ≈ 50 % for single-mask systems. Also, the quasi-triangular modulation shape is not as efficient as that of the (square wave) single-grid systems and so results in some loss of signal to noise. As a result, the choice between single and bigrid systems depends on the relative importance of angular resolution and sensitivity and on the most appropriate detector technology for a given application.

Multigrid collimators

The inclusion of additional grids into a bigrid collimator provides another design option. The additional grids suppress the response at intermediate peaks (Figure 12.5). If enough additional grids are inserted, this can provide a system that has only one response peak across the FOV. A single such collimator can be rastered in time or a fixed array of such collimators can be employed, each with its peak response in a (slightly) different direction. In either case, the result is a direct imaging system, effectively equivalent to a conventional focused telescope in that it has multiple detector elements, each of which is sensitive to a specific area on the source. The angular resolution is still determined by the pitch of the collimator grids. The advantage over the single and bigrid systems is that no image reconstruction is required and so the signal from strong sources does not affect the detection of weak ones. A significant disadvantage, however, is that the available frontal area of the instrument must be shared by many small subcollimators, each with its own look-direction. Alternatively, for scanned systems, a given source is observed with a low duty cycle. In either case, the sensitivity to any given source in the FOV can be very low. The HXIS instrument on *SMM* (van Beek et al 1980) provides a good example of this approach.

Grids

Several technologies have been used to fabricate the grid or mask 'optics' of collimator systems. For coarse grids, mechanical assembly of conventionally machined parts is the typical choice (e.g., Figure 12.2). At intermediate pitches (down to ≈ 1 mm) electron discharge machining is a viable option (e.g., Crannell et al 1991). For fine grids, stacking of photo-etched grid layers (Figure 12.6) has been used to achieve pitches of 35 μm in 1 mm thick material (Lin et al 2002).

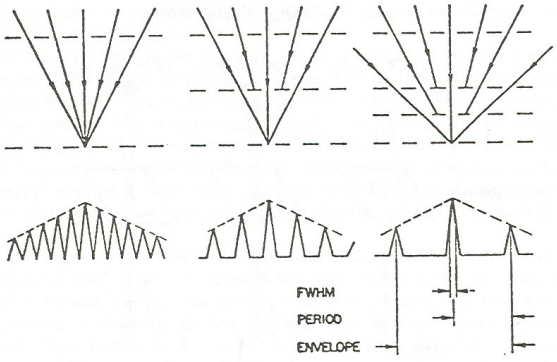

Figure 12.5: Top: Possible photon paths for bigrid and multiple grid collimators, illustrating the periodic maxima in their response and the effect of intermediate grids. Bottom: Corresponding plots of the effective area as a function of incident angle. For a given collimator length, the angular resolution is given by the ratio $\frac{1}{2}$ grid pitch/separation; the response envelope (FOV) is defined by the detector and grid size. The intermediate grids affect the period.

The performance of any collimator or mask system is also subject to two physical limitations. The first limitation is set by a combination of three factors. Specifically, the minimum thickness of the grid is determined by the requirement that the grid be opaque at the maximum energy of interest. This thickness constrains the FOV to an angle given by the ratio of slit width/grid thickness. The slit width in turn is closely tied to the angular resolution ($\frac{1}{2}$ slit pitch / separation). For a collimator of a given length, this combination of factors imposes an unavoidable physics-driven tradeoff among angular resolution, FOV and maximum energy.

The second limitation is diffraction. This sets a lower limit to the energy range since at lower energies the front grid can function as a diffraction grating. A complete analysis of the diffraction response of multigrid collimators (Lindsey 1978) was simplified by Crannell et al (1991) for the case of a bigrid collimator.

Both of these limitations can be relevant in practice. For example, *RHESSI*'s angular resolution above $\approx$ 1 MeV is limited to $35''$ by a requirement that it maintain a 1° FOV. With a 1.55 m long collimator, *RHESSI* is also prevented from achieving $2.3''$ resolution below 4 keV by diffraction.

Alignment and aspect

The significance of internal alignment and tolerance issues depends on the type of mask or collimator system employed. For mask systems with two-dimensional detectors, the primary requirement is that the relative positions of the mask and detector be known in inertial coordinates to an accuracy small compared to the angular resolution. This must be achieved on timescales that are longer than both the integration time and aspect cadence. The requirement can be met if both the

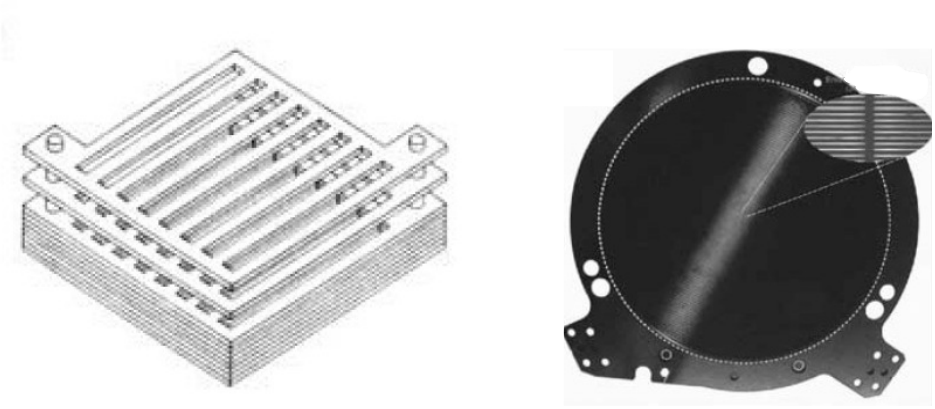

Figure 12.6: Left: Schematic illustration of stacking photo-etched layers to achieve a thick grid with fine slits. Right: *RHESSI* 9 cm diameter, 1 mm thick grid whose slits (inset) have a 35 μm period. The FOV is $\approx 1^\circ$ (from Lin et al 2002).

metering structure and pointing platform are stable. Alternatively, one can trade mechanical and pointing stability for data rate by using short binning times and a high-cadence aspect system. For high-resolution bigrid collimators this can be done by embedding key elements of the aspect system in the plane of the grids (e.g., Zehnder et al 2003). In this way mechanical flexure of the intermediate metering structure is equivalent to a variation in pointing. With photon tagging or short integration times and a high-cadence aspect system, such variations can then be fully compensated for during analysis.

For bigrid collimators, there is an additional requirement in that the top and bottom grid slits must be parallel (viz., that their relative twist be maintained). However the twist requirement is much coarser than the angular resolution since the former is determined by the ratio of grid pitch to grid diameter (and not to the grid separation). For example, *RHESSI* achieved $2''$ imaging with internal alignment that was controlled to $\approx 1'$ and pointing that was controlled to several minutes of arc. This use of knowledge in place of control of the pointing and internal alignment can greatly simplify the mechanical implementation of a high-resolution collimator.

The alignment requirements for multigrid collimators are much more severe since the intermediate grids must be positioned and maintained to a precision that is small compared to the grid pitch. This requirement was met, however, by the HXIS instrument on *SMM* with grid apertures ≈ 25 μm.

Summary and outlook

Grids and masks have provided the basis for X-ray and γ-ray imaging since the 1960s (Bradt et al 1992). (Also see the list of missions found at http://astrophysics.gsfc.nasa.gov/cai/coded_inss.html). Table 12.1 summarizes the characteristics of a

Table 12.1: Representative instruments.

Mission/ instrument	Year	E_x/keV	Prime imaging objective	Imager type(s)	Area A/cm^2	FWHM resolution	Reference
Ariel-5/ B	1974–1980	0.9 to 18	survey	scanner	≈ 290	0.75°	Villa et al 1976
SMM/ HXIS	1980–1989	3.5 to 30	solar flares	multigrid direct imaging	0.07	$8''$	van Beek et al 1980
Yohkoh/ HXT	1991–2001	15 to 100	solar flares	64 bi-grid collimators	70	$8''$	Kosugi et al 1991
HETE-2/ WXM	2000–present	2 to 25	burst location	two 1-D random masks	350	$\approx 10'$	Kawai et al 1999
INTEGRAL/ IBIS	2002–present	15 to 10 000	source identification	URA	2500	$12'$	Ubertini et al 2003
RHESSI	2002–present	3 to 17 000	solar flares	9 RMCs	90	$2.3''$	Lin et al 2002
Swift/ BAT	2004–present	15 to 150	burst location	URA	5200	$17'$	Barthelemy et al 2005

representative set of such instruments. Their capabilities have grown as grid and detector technologies have improved. The techniques do have some significant disadvantages, however. The design requirement that the detector area be comparable to that of the grid or mask makes it much more difficult to reduce background for applications that require high sensitivity. Sensitivity is further affected since the telescope mask or collimator intentionally blocks about half to three quarters of the incident photon flux. In source-limited situations where background is not an issue, the ability to detect weak sources in the presence of strong ones can be limited by the fact that all sources contribute noise to the detection of each source component. Image quality is also significantly constrained for morphologically rich sources.

In the coming years, we can expect masks and collimators to be partially supplanted by technical developments in grazing-incidence optics, especially in low energy applications that require only intermediate resolution and narrow FOVs. In such contexts, focusing optics has a commanding advantage where sensitivity and background rejection are the main drivers or where morphologically complex sources need be imaged.

Nevertheless there will continue to be many applications where mask and grid-based imaging is appropriate. As we have seen, the technique can be adapted to platforms which are three-axis stabilized, rotating or badly pointed (as with balloons); it can be implemented in a wide range of size scales, from compact designs of a few centimeters in scale, to configurations requiring extended booms on scales

of meters; it can provide angular resolutions from seconds of arc to degrees over FOVs from $\approx 1^\circ \times 1^\circ$ to ≈ 1 sr; and for a given instrument, the same 'optics' can be used over a wide range of energies, a feature that greatly aids co-location of images and imaging spectroscopy. Therefore, in applications where either compactness, low mass, wide FOV or high-energy response is required, masks, grids and collimators will continue to provide the imaging technique of choice.

Acknowledgement

This work was supported by NASA Contract NAS5-98033.

Bibliography

Barthelemy SD and the *Swift* Instrument Team (2005) Burst alert telescope (BAT) on the *Swift* MIDEX mission. Space Sci Rev 120:143–164

Bradt HVD, Ohashi T, Pounds KA (1992) X-ray astronomy missions. Ann Rev Astron Astrophys 30:391–427

Crannell CJ, Dennis B, Orwig L (plus eight authors) (1991) A balloon-borne payload for imaging hard X-rays and gamma rays from solar flares. AIAA-91-3653:1–11

Dicke RH (1968) Scatter-hole cameras for X-rays and gamma rays. Astrophys J 153:L101–106

Fenimore EE (1980) Coded aperture imaging: the modulation transfer function for uniformly redundant arrays. Appl Opt 19:2465–2471

Hurford GJ, Schmahl EJ, Schwartz RA (plus 11 authors) (2002) The *RHESSI* imaging concept. Sol Phys 210:61–86

Kawai N Matsuoka M, Yoshida A (plus seven authors) (1999) Wide-field X-ray monitor on *HETE-2*. Astron Astrophys Suppl Ser 138:563–564

Kosugi T, Makishima K, Murakami T (plus nine authors) (1991) The Hard X-ray Telescope (HXT) for the *Solar-A* Mission. Solar Phys 136:17–36

Lin RP, Dennis BR, Hurford GJ (plus 63 authors) (2002) The Reuven Ramaty high-energy solar spectroscopic imager (*RHESSI*). Sol Phys 210:3–32

Lindsey CA (1978) Effects of diffraction in multiple-grid telescopes for X-ray astronomy. J Opt Soc Am 68:1708–1715

Makishima K, Miyamoto S, Murakami T (plus four authors) (1977) Modulation collimator as an imaging device, in K A van der Hucht and G Vaiana (eds), New Instrumentation for Space Astronomy, Pergamon Press, New York, pp 277–289

Mertz L (1968) A dilute image transform with application to an X-ray star camera. Proc Symp Mod Opt 17:787–791

Oda M (1965) High-resolution X-ray collimator with broad field of view for astronomical use. Appl Optics 4:143–143

Prince TA, Hurford GJ, Hudson HS, Crannell CJ (1988) Gamma-ray and hard X-ray imaging of solar flares. Sol Phys 118:269–290

Ramsey BD, Austin RA, Decher R (1993) Instrumentation for X-ray astronomy. Space Sci Rev 69:139–204

Schmahl EJ, Hurford GJ (2002) *RHESSI* observations of the size scales of solar hard X-ray sources. Sol Phys 210:273–286

Schnopper HW, Thompson RI, Watt S (1968) Predicted performance of a rotating modulation collimator for locating celestial X-ray sources. Space Sci Rev 8:534–542

Ubertini P, Lebrun F, Di Cocco G (plus 17 authors) (2003) IBIS: The imager on-board *INTEGRAL*. Astronom Astrophys 411:L131–139

van Beek HF, Hoyng P, Lafleur B, Simnett GM (1980) The hard X-ray imaging spectrometer (HXIS). Sol Phys 65:39–52

Villa G, Page CG, Turner MJL (plus three authors) (1976) The Ariel V sky survey instrument and new observations of the Milky Way. Mon Not Roy Astronom Soc 176:609–620

Zehnder A, Bialkowski J, Burri F (plus 12 authors) (2003) *RHESSI* imager and aspect systems. Proc SPIE 4853:41–59